Electronic Supplementary Information (ESI†)

Inducing Atomically Dispersed Cl-FeN_4 Sites for ORR in the SiO_2-Mediated Synthesis of Highly Mesoporous N-enriched C-networks

Xiong Zhang,[a] Lai Truong-Phuoc,[a] Xuemei Liao,[a,b,] Vasiliki Papaefthimiou,[a] Matteo Pugliesi,[c] Giulia Tuci,[c] Giuliano Giambastiani,[a,c,]* Sergey Pronkin,[a,]* Cuong Pham-Huu [a,]**

[a] *Institute of Chemistry and Processes for Energy, Environment and Health (ICPEES), ECPM, UMR 7515 CNRS-University of Strasbourg, 25 rue Becquerel, 67087 Strasbourg Cedex 02, France.* giambastiani@unistra.fr, sergey.pronkin@unistra.fr, cuong.pham-huu@unistra.fr

[b] *School of Food and Biological Engineering, Xihua University, 610039, Chengdu, China.* xmliao@mail.xhu.edu.cn

[c] *Institute of Chemistry of OrganoMetallic Compounds, ICCOM-CNR and Consorzio INSTM, Via Madonna del Piano, 10 – 50019, Sesto F.no, Florence, Italy.* giuliano.giambastiani@iccom.cnr.it

Contents

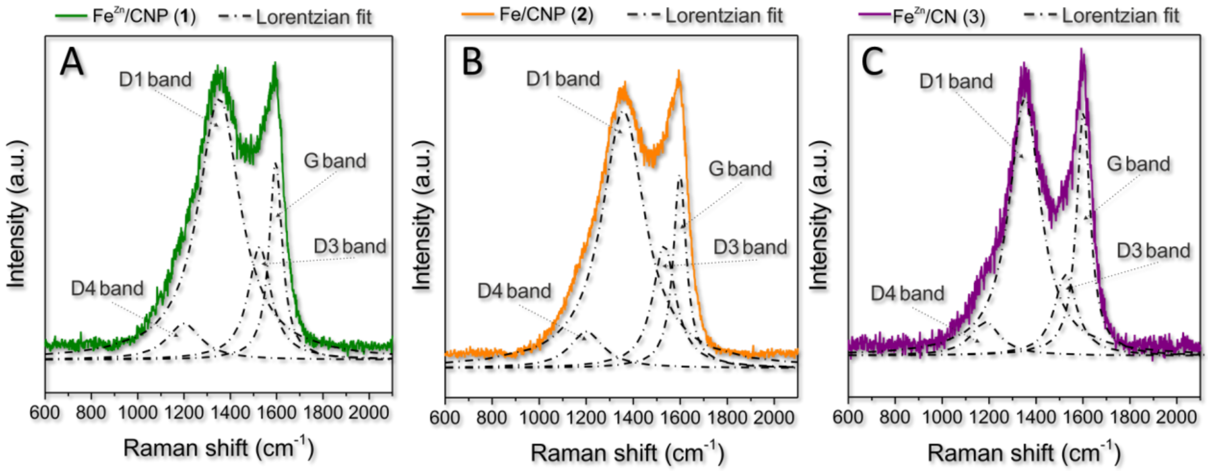

Fig. S1†. Raman spectra of samples **1-3** along with their relative Lorentzian peaks fitting (dashed lines). I_D/I_G values are reported in Table 1.

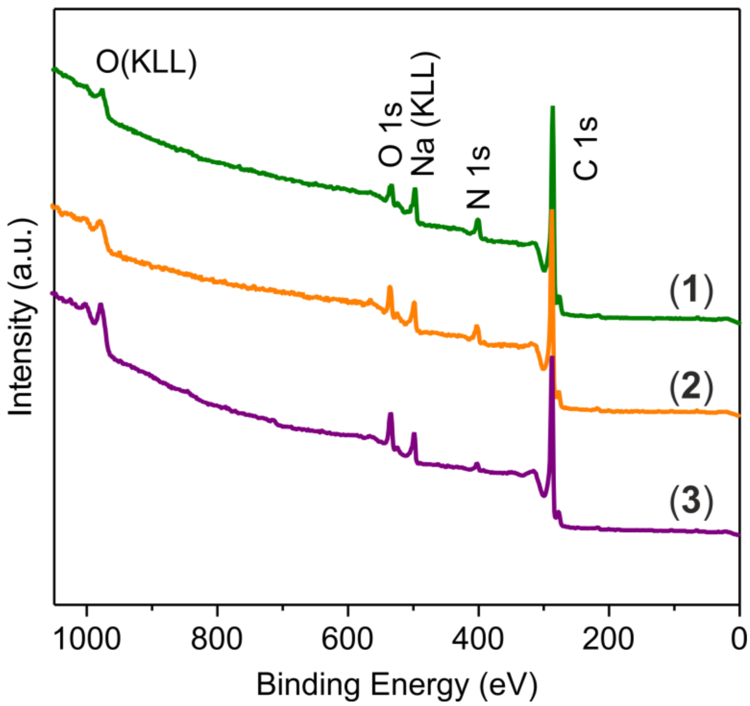

Fig. S2†. XPS survey spectra of Fe^{Zn}/CNP (**1**), and Fe/CNP (**2**) and Fe^{Zn}/CNP (**3**). All spectra contain the Auger line of Na KLL caused by the material treatment with a NaOH solution for the silica template removal.[1]

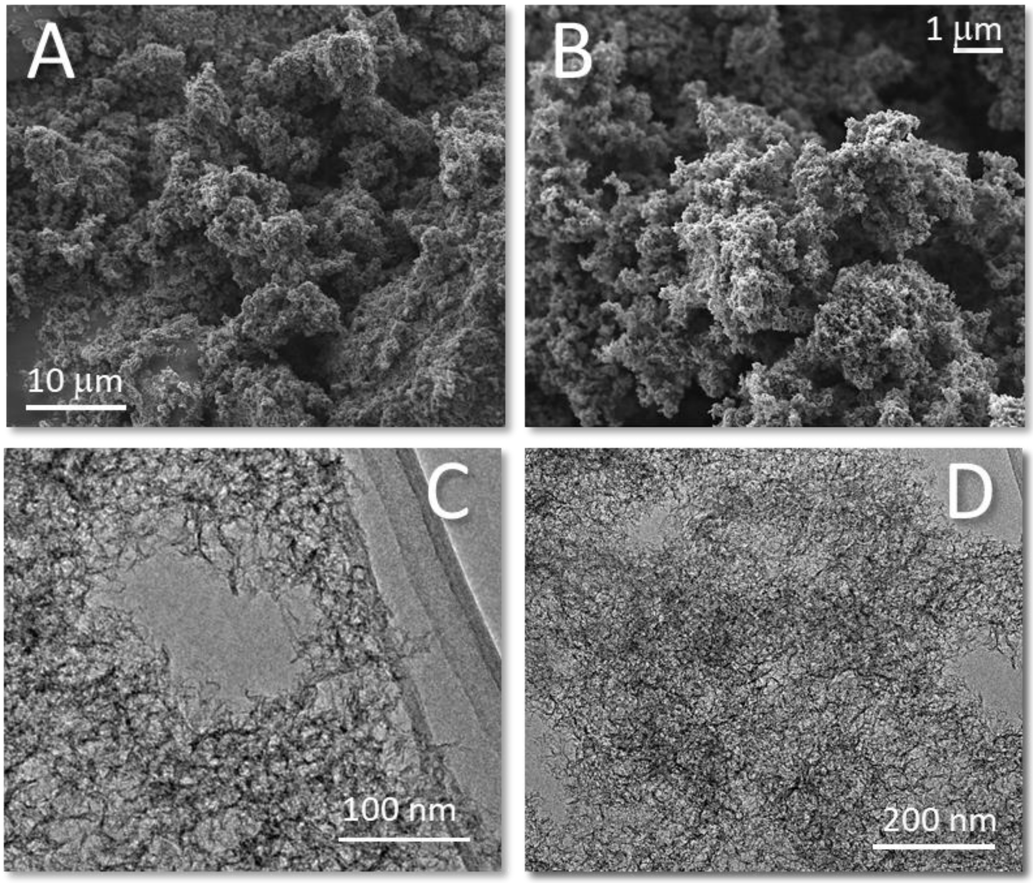

Fig. S3†. A-B) SEM and C-D) TEM images of **1** at different magnifications

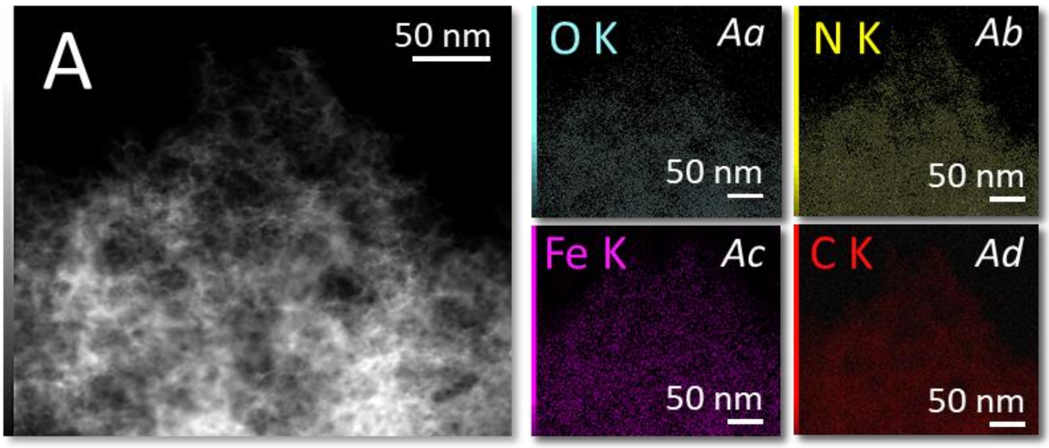

Fig. S4†. A) HAADF-STEM image of **1** along with corresponding EDX elemental mapping (Aa-Ad) Color codes: C (red), N (yellow), O (light blue) and Fe (pink).

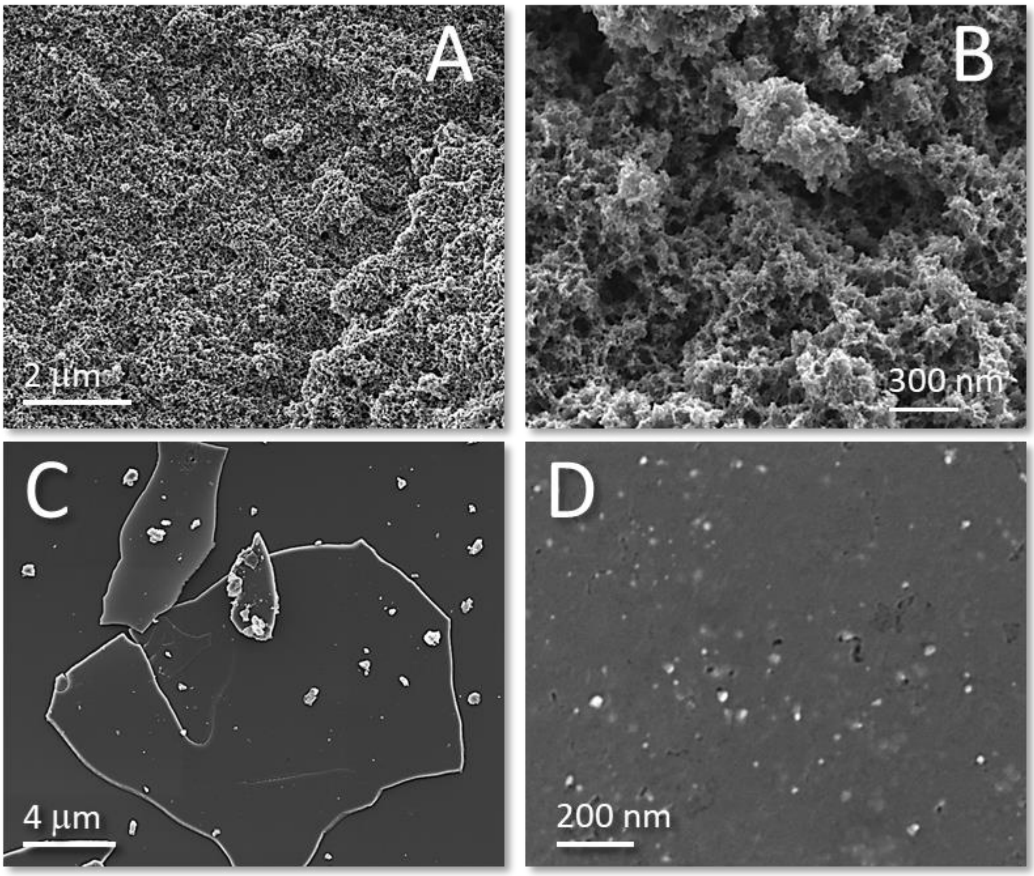

Fig. S5†. SEM images of 2 (A,B) and 3 (C,D) at different magnifications.

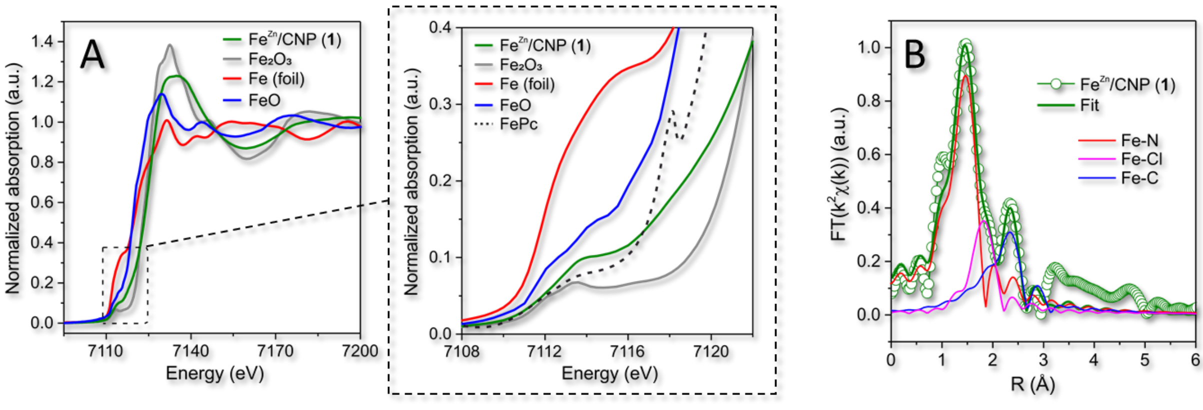

Fig. S6†. A) Normalized XANES spectra at the Fe K-edge of **1**, metallic Fe foil, FeO and Fe_2O_3 along with a magnification of the pre-edge transition peaks. Expansion on the right-side hand also include the pre-edge peak of a Fe-phthalocyanine (FePc) as a FeN_4 structure in a typical square-planar configuration with high D_{4h} symmetry. B) EXAFS fitting curve of **1** in R space with all components. No phase-shift correction was applied to the Fourier transforms.

Table S1†. Structural data from the fitting of Fe K-edge EXAFS signal in Fe^{Zn}/CNP (**1**).

Path	Coord. Numb.	R(Å)[a]	σ^2 (10^{-2} Å^2)[b]	ΔE_0 [c]	R-factor [d]
Fe-N	3.4 ± 0.2	1.97 ± 0.01	2.9 ± 0.9	-2.8 ± 0.4	0.009
Fe-Cl	1.0 ± 0.1	2.32 ± 0.01	2.7 ± 1.2	4.6 ± 0.9	-
Fe-C	4.8 ± 0.6	2.90 ± 0.01	3.8 ± 1.9	-2.8 ± 0.4	-

[a] Interatomic distance. [b] Debye-Waller factor. [c] Difference in the threshold Fermi level between data and fit. [d] Goodness of fit parameters.

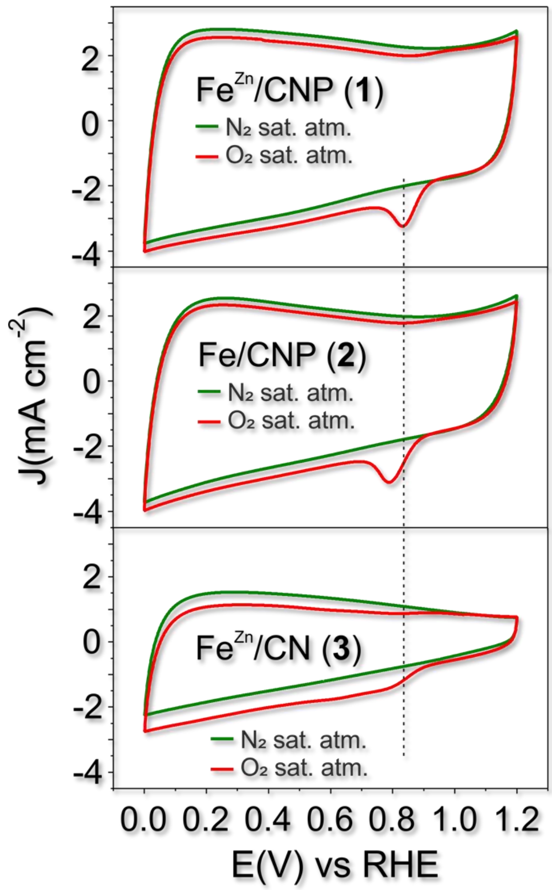

Fig. S7†. Cyclic voltammograms of samples **1-3** recorded under N_2-saturated (green lines) and O_2-saturated solutions (red lines). The potential was linearly swept from 0.0 to 1.2 V at a scan rate of 50 mV s^{-1} vs. RHE as reference electrode in a water 0.1 M KOH electrolyte solution.

Table S2†. Number of exchanged electrons (n_E) for RRDE measurements carried out at different catalyst loadings (188, 377 and 755 μg cm^{-2}).

Catalyst loading (μL of ink)	8	16	32
Catalyst loading (μg cm^{-2})	188	377	755
Catalyst loading (μg)[a]	37	74	148
Exchange electrons (*n*)	3.22	3.75	3.57

[a] 0.19625 cm^2 GC rotating-disk electrode

Table S3†. Selection of the most representative Fe-SACs of the *state-of-the-art* reported in the literature so far and their ORR performance under alkaline environment.

Entry	Catalyst	Fe content (wt.%)[a]	Mass loading (mg cm^{-2})	E_{on} (V)[b]	$E_{1/2}$ (V)[b]	J_L (mA cm^{-2})	Tafel slope (mV dec^{-1})	Ref.
1	Fe^{Zn}/CNP (**1**)	0.40	0.38	0.97	0.88	6.35	39.5	**this work**
2	Fe-N-HMCTs		0.20	0.99	0.87	5.66	89	2
3	Fe-N_x-C-1		0.68	0.93	0.85	6.5	74	3
4	ICM-$FePhen_3$		0.80	0.91[c]	0.86	5.8[c]		4
5	FN-800		0.70	0.93	0.82	5.4[c]		5
6	m-Fe/N/C-900		0.6		0.84	5.8		6
7	Fe-NC-S	1.93	0.2	0.96	0.88	5.7	49	7
8	Fe/NSCN	2.54	0.75	1.09	0.88	5.08	92	8
9	FeNC-900		0.7	0.98[c]	0.85	5.6		9
10	FeBNC-800	0.40	0.6	0.97	0.84	5.51	69	10
11	Fe@Aza-PON		0.28	0.9[c]	0.84	6[c]	60	11
12	Fe-ISA/SNC	0.947	0.51	0.96	0.90	5.7[c]	44	12
13	Fe-SAs/NPS-HC	1.54	0.5	0.96[c]	0.91	6[c]	36	13
14	Fe-SilkPNC	0.12	0.6	0.95	0.85	5[c]	61.4	14
15	Fe/N/S-PCNT		0.1	0.96	0.84	5[c]		15
16	Fe-NMP		0.6	0.97	0.84	4.8[c]		16
17	SAFe-NDC-H	1.15	0.4	0.92[c]	0.86	5[c]	61	17
18	3DOM FeNC-900	1.59	0.6	0.96[c]	0.88	6[c]	49	18
19	C-FeZIF-1.44-950		0.5	0.95[c]	0.86	6.4[c]		19
20	Fe-NSDC		0.1	0.96	0.84	5.5[c]	56	20
21	Fe_3C/Fe@G-800	52.8	0.6	0.94	0.80	4.8[c]		21
22	Fe–N–C/rGO		0.35	0.94	0.81	6[c]	98.8	22
23	SA-Fe-HPC		0.1	0.96[c]	0.89	5.4	49	23
24	Fe–N–C/MXene		0.1	0.92	0.84	6[c]		24
25	Fe@N–C NT/NSs		0.25	1.00	0.82	7.5[c]	69.6	25
26	Fe-SAs/NSC	0.87	0.2	1	0.87	6[c]	60	26
27	C-FeHZ8@g-C_3N_4-950		0.5	0.92[c]	0.85	5.5[c]		27
28	Fe-N/P-C-700		0.6	0.94	0.87	5.66		28
29	SC-Fe		0.25	0.96[c]	0.87	5.8[c]	51.3	29
30	meso-Fe–N–C	2.9	0.4	0.92[c]	0.85	5.2[c]		30

31	Fe–N/C-155	5.86	0.245	1.09	0.85	6.5		31
32	Fe(0)@FeNC	0.5	0.3	0.95	0.85	6.4	72	32
33	Fe-LC-900	4.13	-	0.96	0.82	5 [c]	74	33
34	Fe–N–CPNS		0.2	0.92 [c]	0.84	5.8		34
35	Fe-CNSs-N		0.31	0.95	0.84	5.2 [c]	70.6	35
36	Fe-N-3DPC-1000	0.87	0.2	0.96 [c]	0.85	4.8 [c]	79	36
37	Fe/OES	0.11	0.4	1.00	0.85	6.1 [c]		37
38	1/CNT		0.08	0.93	0.84	5 [c]	84	38
39	3D-FePDC		-	0.98	0.84	5.5 [c]	81	39
40	Fe_3C–FeN/NC-2	0.44	0.4	0.95	0.8	5.1	55	40
41	FeS/Fe_3C@NS-C-900		0.1156	1.03	0.78	6.83	94	41
42	Fe1-HNC-500-850	0.31	0.2	0.93 [c]	0.84	5.80	51.5	42
43	Fe3-NG		0.5	1.03	0.84	7.0 [c]		43
44	Fe-N-CC	0.7	0.1	0.94	0.83	4.4 [c]		44
45	S-Fe/N/C		0.16	0.91	0.84	5.1 [c]		45

[a] as measured from ICP analyses [b] potential values reported *vs*. RHE [c] as extrapolated from figures in the corresponding manuscript.

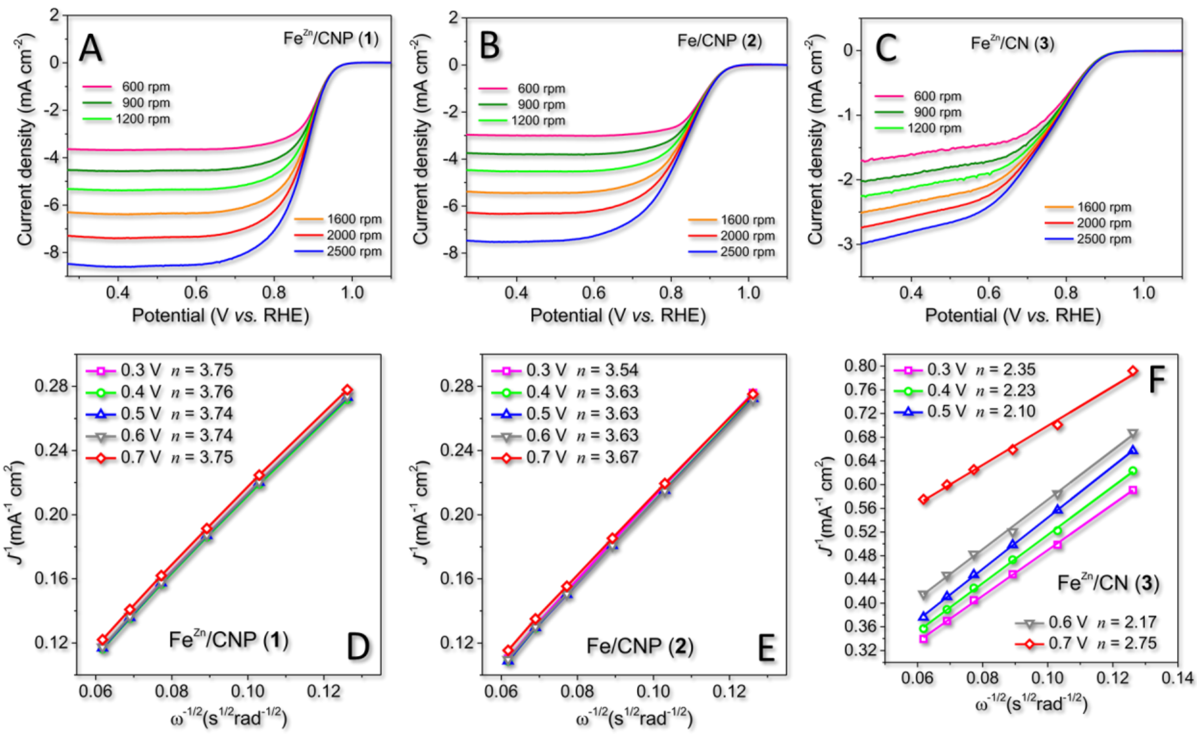

Fig. S8†. (A-C) Linear sweep voltammograms (LSVs) and (D-F) K-L plots for ORR in O_2-saturated 0.1 M KOH solution promoted by Fe^{Zn}/CNP (**1**), Fe/CNP (**2**) and Fe^{Zn}/CN (**3**) at variable spin rates (600, 900, 1200, 1600, 2000 and 2500 rpm). Scan rates: 10 mV s^{-1}, catalyst loading 377 μg cm^{-2} for each catalyst at work.

References:

1. R. Ma, G. Lin, Q. Ju, W. Tang, G. Chen, Z. Chen, Q. Liu, M. Yang, Y. Lu and J. Wang, *Appl. Catal. B-Environ.*, 2020, **265**, 118593.
2. X. Cui, L. Gao, S. Lei, S. Liang, J. Zhang, C. D. Sewell, W. Xue, Q. Liu, Z. Lin and Y. Yang, *Adv. Funct. Mater.*, 2021, **31**, 2009197
3. Y. Liu, B. Huang, X. Zhang, X. Huang and Z. Xie, *Journal of Power Sources*, 2019, **412**, 125-133.
4. J. Li, Q. Jia, S. Mukerjee, M.-T. Sougrati, G. Drazic, A. Zitolo and F. Jaouen, *Catalysts*, 2019, **9**, 144.
5. X. Yan, Y. Yao and Y. Chen, *Nanoscale research letters*, 2018, **13**, 1-7.
6. C. Guo, Y. Li, Z. Li, Y. Liu, Y. Si and Z. Luo, *Nanoscale research letters*, 2020, **15**, 1-14.
7. X. Li, C.-S. Cao, S.-F. Hung, Y.-R. Lu, W. Cai, A. I. Rykov, S. Miao, S. Xi, H. Yang and Z. Hu, *Chem*, 2020, **6**, 3440-3454.
8. X. Zhang, L. Truong-Phuoc, X. Liao, G. Tuci, E. Fonda, V. Papaefthymiou, S. Zafeiratos, G. Giambastiani, S. Pronkin and C. Pham-Huu, *ACS Catal.*, 2021, **11**, 8915-8928.
9. W.-J. Jiang, W.-L. Hu, Q.-H. Zhang, T.-T. Zhao, H. Luo, X. Zhang, L. Gu, J.-S. Hu and L.-J. Wan, *Chem Commun*, 2018, **54**, 1307-1310.
10. K. Yuan, S. Sfaelou, M. Qiu, D. Lützenkirchen-Hecht, X. Zhuang, Y. Chen, C. Yuan, X. Feng and U. Scherf, *ACS Energy Letters*, 2017, **3**, 252-260.
11. S.-J. Kim, J. Mahmood, C. Kim, G.-F. Han, S.-W. Kim, S.-M. Jung, G. Zhu, J. J. De Yoreo, G. Kim and J.-B. Baek, *Journal of the American Chemical Society*, 2018, **140**,

1737-1742.

12. Q. Li, W. Chen, H. Xiao, Y. Gong, Z. Li, L. Zheng, X. Zheng, W. Yan, W. C. Cheong and R. Shen, *Advanced materials*, 2018, **30**, 1800588.
13. Y. Chen, S. Ji, S. Zhao, W. Chen, J. Dong, W.-C. Cheong, R. Shen, X. Wen, L. Zheng and A. I. Rykov, *Nature communications*, 2018, **9**, 1-12.
14. C. Wang, W. Chen, K. Xia, N. Xie, H. Wang and Y. Zhang, *Small*, 2019, **15**, 1804966.
15. Z. Tan, H. Li, Q. Feng, L. Jiang, H. Pan, Z. Huang, Q. Zhou, H. Zhou, S. Ma and Y. Kuang, *Journal of materials chemistry A*, 2019, **7**, 1607-1615.
16. M. M. Hossen, K. Artyushkova, P. Atanassov and A. Serov, *Journal of Power Sources*, 2018, **375**, 214-221.
17. W. Ni, Y. Gao, Y. Zhang, H. A. Younus, X. Guo, C. Ma, Y. Zhang, J. Duan, J. Zhang and S. Zhang, *ACS applied materials & interfaces*, 2019, **11**, 45825-45831.
18. X. Zhang, X. Han, Z. Jiang, J. Xu, L. Chen, Y. Xue, A. Nie, Z. Xie, Q. Kuang and L. Zheng, *Nano Energy*, 2020, **71**, 104547.
19. Y. Deng, B. Chi, J. Li, G. Wang, L. Zheng, X. Shi, Z. Cui, L. Du, S. Liao and K. Zang, *Advanced Energy Materials*, 2019, **9**, 1802856.
20. J. Zhang, M. Zhang, Y. Zeng, J. Chen, L. Qiu, H. Zhou, C. Sun, Y. Yu, C. Zhu and Z. Zhu, *Small*, 2019, **15**, 1900307.
21. A. Song, L. Cao, W. Yang, Y. Li, X. Qin and G. Shao, *ACS Sustainable Chemistry & Engineering*, 2018, **6**, 4890-4898.
22. C. Zhang, J. Liu, Y. Ye, Z. Aslam, R. Brydson and C. Liang, *ACS applied materials & interfaces*, 2018, **10**, 2423-2429.

23. Z. Zhang, J. Sun, F. Wang and L. Dai, *Angewandte Chemie*, 2018, **130**, 9176-9181.

24. L. Jiang, J. Duan, J. Zhu, S. Chen and M. Antonietti, *ACS nano*, 2020, **14**, 2436-2444.

25. X. Li, L. Ni, J. Zhou, L. Xu, C. Lu, G. Yang, W. Ding and W. Hou, *Nanoscale*, 2020, **12**, 13987-13995.

26. J. Zhang, Y. Zhao, C. Chen, Y.-C. Huang, C.-L. Dong, C.-J. Chen, R.-S. Liu, C. Wang, K. Yan and Y. Li, *Journal of the American Chemical Society*, 2019, **141**, 20118-20126.

27. Y. Deng, B. Chi, X. Tian, Z. Cui, E. Liu, Q. Jia, W. Fan, G. Wang, D. Dang and M. Li, *Journal of Materials Chemistry A*, 2019, **7**, 5020-5030.

28. K. Yuan, D. Lützenkirchen-Hecht, L. Li, L. Shuai, Y. Li, R. Cao, M. Qiu, X. Zhuang, M. K. Leung and Y. Chen, *Journal of the American Chemical Society*, 2020, **142**, 2404-2412.

29. J. Xie, B. Q. Li, H. J. Peng, Y. W. Song, J. X. Li, Z. W. Zhang and Q. Zhang, *Angewandte Chemie International Edition*, 2019, **58**, 4963-4967.

30. Y. Zhou, Y. Yu, D. Ma, A. C. Foucher, L. Xiong, J. Zhang, E. A. Stach, Q. Yue and Y. Kang, *ACS Catalysis*, 2020, **11**, 74-81.

31. G. Ye, Q. He, S. Liu, K. Zhao, Y. Su, W. Zhu, R. Huang and Z. He, *Journal of Materials Chemistry A*, 2019, **7**, 16508-16515.

32. Z. Li, L. Wei, W.-J. Jiang, Z. Hu, H. Luo, W. Zhao, T. Xu, W. Wu, M. Wu and J.-S. Hu, *Applied Catalysis B: Environmental*, 2019, **251**, 240-246.

33. R. Soni, S. N. Bhange and S. Kurungot, *Nanoscale*, 2019, **11**, 7893-7902.

34. G. Wang, J. Deng, T. Yan, J. Zhang, L. Shi and D. Zhang, *Nanoscale*, 2020, **12**, 5601-5611.

35. Y. Wang, R. Gan, H. Liu, M. Dirican, C. Wei, C. Ma, J. Shi and X. Zhang, *Journal of Materials Chemistry A*, 2021, **9**, 2764-2774.
36. Y. Huang, K. Liu, S. Kan, P. Liu, R. Hao, W. Liu, Y. Wu, H. Liu, M. Liu and K. Liu, *Carbon*, 2021, **171**, 1-9.
37. C. C. Hou, L. Zou, L. Sun, K. Zhang, Z. Liu, Y. Li, C. Li, R. Zou, J. Yu and Q. Xu, *Angewandte Chemie*, 2020, **132**, 7454-7459.
38. L. Xie, X. P. Zhang, B. Zhao, P. Li, J. Qi, X. Guo, B. Wang, H. Lei, W. Zhang and U. P. Apfel, *Angewandte Chemie International Edition*, 2021, **60**, 7576-7581.
39. P. K. Gangadharan, A. Pandikassala and S. Kurungot, *ACS Applied Materials & Interfaces*, 2021, **13**, 8147-8158.
40. F. Zhou, P. Yu, F. Sun, G. Zhang, X. Liu and L. Wang, *Journal of Materials Chemistry A*, 2021, **9**, 6831-6840.
41. Y.-W. Li, W.-J. Zhang, J. Li, H.-Y. Ma, H.-M. Du, D.-C. Li, S.-N. Wang, J.-S. Zhao, J.-M. Dou and L. Xu, *ACS Applied Materials & Interfaces*, 2020, **12**, 44710-44719.
42. X. Zhang, S. Zhang, Y. Yang, L. Wang, Z. Mu, H. Zhu, X. Zhu, H. Xing, H. Xia and B. Huang, *Advanced Materials*, 2020, **32**, 1906905.
43. X. Cui, S. Yang, X. Yan, J. Leng, S. Shuang, P. M. Ajayan and Z. Zhang, *Advanced Functional Materials*, 2016, **26**, 5708-5717.
44. G. A. Ferrero, K. Preuss, A. Marinovic, A. B. Jorge, N. Mansor, D. J. Brett, A. B. Fuertes, M. Sevilla and M.-M. Titirici, *ACS nano*, 2016, **10**, 5922-5932.
45. K. Hu, L. Tao, D. Liu, J. Huo and S. Wang, *ACS applied materials & interfaces*, 2016, **8**, 19379-19385.